Spin Polarized Tunneling and Injection in Semiconductors and Oxides

Ingrid Mertig, Chairman

Spin-polarized electron transport in ferromagnet/semiconductor hybrid structures (invited)

J. A. C. Bland,[a] A. Hirohata, C. M. Guertler, Y. B. Xu, and M. Tselepi
Cavendish Laboratory, University of Cambridge, Madingley Road, Cambridge CB3 0HE, England

Two major problems in spin electronics remain to be solved: room temperature spin injection at a source *and* spin detection at a drain electrode. The lateral size of magnetic contacts and the presence of a potential barrier at the interface are believed to have a key influence on the efficiency of both of these processes. We therefore aimed to clarify these issues by studying spin-polarized transport across epitaxially grown single crystal Fe (001)/GaAs nanoclusters and at the Schottky barrier formed at $Ni_{80}Fe_{20}$/GaAs interfaces. We observed a negative contribution to the magnetoresistance of an ultrathin (2.5 ML) discontinuous epitaxial Fe film as occurs in tunnel magnetoresistance. This result suggests that spin transport via GaAs is possible on the nanoscale. In the continuous NiFe/GaAs structures, circularly polarized light was used to create a population of spin-polarized electrons in the GaAs substrate and spin-polarized electron transport across the interface at room temperature was detected as an electrical response associated with the field-dependent photocurrent. Surprisingly, highly efficient spin transmission is observed at room temperature, indicating that there is no significant loss of spin polarization for electrons crossing the interface. This result unambiguously demonstrates that spin detection is possible at room temperature in a continuous ferromagnet/semiconductor contact in the presence of the Schottky barrier. © *2001 American Institute of Physics.* [DOI: 10.1063/1.1361045]

I. INTRODUCTION

The study of conduction electron spin transport in metals has led to new classes of electronic devices based on the manipulation of the electron spin. Highly sensitive magnetic field sensors are used in today's read heads and integrated digital devices are being developed for high speed and low power applications.[1,2] Proposed spin analogues to conventional semiconductor (SC) devices have recently stimulated great interest, e.g., the spin-polarized field effect transistor (spin FET)[3] and the spin-polarized light-emitting diode.[4–6] As originally demonstrated in metals,[7,8] and applied to the spin FET,[3] spin electronic devices involve: (i) the injection of spin-polarized carriers at a magnetic/nonmagnetic material interface; (ii) the transmission of polarized carriers in the nonmagnetic material; and (iii) the detection of polarized carriers as a voltage (or current) modulation at a nonmagnetic/magnetic material interface (see Fig. 1).

Recent optical experiments[4–6] demonstrated the injection of spins in magnetic/nonmagnetic SC structures. The polarized carriers diffused into the nonmagnetic SC for a length that was adequate to permit their observation by electroluminescence. In these cryogenic experiments, spin-dependent signals were not observed above 40 K, and the experimental observation of a relatively large polarization[4] required magnetic fields of order 3 T. In addition, fundamental obstacles to achieving efficient spin transmission across ferromagnetic metal/SC interfaces have recently been raised.[9,10] The spin injection from a ferromagnet (FM) directly into a SC is still a great challenge. The converse effect (iii), furthermore, remains to be shown, even though the spin detection is as important as the spin injection.

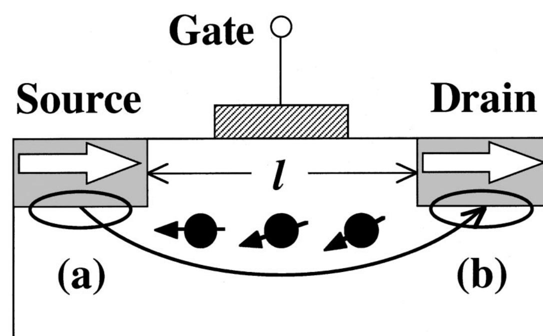

FIG. 1. Schematic diagram of a proposed spin FET. The successful operation of the spin FET requires both: (a) spin injection at the source and (b) spin detection at the drain. Both of these processes depend crucially on the electronic properties of the interface. The lateral separation *l* of the two contacts is likely to be of key importance.

[a]Author to whom correspondence should be addressed; electronic mail: jacb1@phy.cam.ac.uk

 © 2001 American Institute of Physics

Downloaded 28 Nov 2002 to 144.32.136.70. Redistribution subject to AIP license or copyright, see http://ojps.aip.org/japo/japcr.jsp

In this study, we focus on the issues of lateral size (compared to the spin coherence length) and the presence of a potential barrier at the interface and, in this context, report on both the transport properties of epitaxial Fe nanoclusters grown on atomically clean semi-insulating GaAs (100) substrates and the detection of polarized carriers as a photocurrent modulation at a FM/SC interface. In the spin tunneling study, the effective nanocluster separation is well below the spin diffusion length giving rise to the possibility of spin-dependent electron transport between magnetic clusters. By using *in situ* magnetoresistance (MR) measurements, we were able to study the temperature characteristics and the evolution of the MR with thickness of 1.0–8.0 ML thick films. For spin detection experiments, we have used circularly polarized light to create a population of spin-polarized electrons in semiconducting GaAs. Their spin-dependent transport across the FM/SC interface is detected as an electrical response associated with the field dependent photocurrent. Surprisingly, highly efficient spin transmission is observed at room temperature, indicating that there is no significant loss of spin polarization for electrons crossing the interface. A change in the photocurrent of up to 20% is observed, and this is expected to increase further for photon energies approaching the GaAs band gap.

II. EXPERIMENTAL PROCEDURE

We used molecular beam epitaxy techniques to fabricate FM layers directly onto GaAs (100) substrates in an ultrahigh vacuum (UHV) chamber with a base pressure of 4×10^{-10} mbar. The FM layers were grown at room temperature at a rate of about 1 ML/min. The deposition rate was monitored by a quartz crystal, which was calibrated by thickness measurements using atomic force microscopy.

For the spin tunneling study, a brief etching of the GaAs in H_2SO_4 solution was performed before loading in the UHV chamber and then annealing to 550 °C for 30 min. At a chosen Fe thickness the growth process was interrupted and MR measurements were carried out at various temperatures ($100\leqslant T\leqslant300$ K). For a detailed description of the experimental setup, see Ref. 11.

In the case of the spin detection measurements, the ohmic contacts on the bottom of the GaAs substrates were prepared by evaporating 100 nm thick GeAuNi and AuBe followed by annealing at 770 K for 2 min for the case of *n*- and *p*-type substrates, respectively. The substrates were cleaned by an oxygen plasma for 2 min before being loaded into the UHV chamber, and then 5 nm thick $Ni_{80}Fe_{20}$ layers were grown directly onto GaAs (100) ($n=10^{23}$, 10^{24}, and $p=10^{25}\ \mathrm{m}^{-3}$) substrates, capped with 3 nm thick Au layers. Two Al contacts (550 nm thick) were evaporated onto the capping layer. Current–voltage ($I-V$) measurements across two Al electrical contacts attached to the top and one ohmic contact to the bottom of the substrate were performed both with and without photoexcitation.[12,13] A circularly polarized laser beam (with the photon energy $h\nu$ in the range $1.59\leqslant h\nu\leqslant2.41$ eV) was then used together with an external magnetic field to investigate the spin dependence of the photocurrent at room temperature.

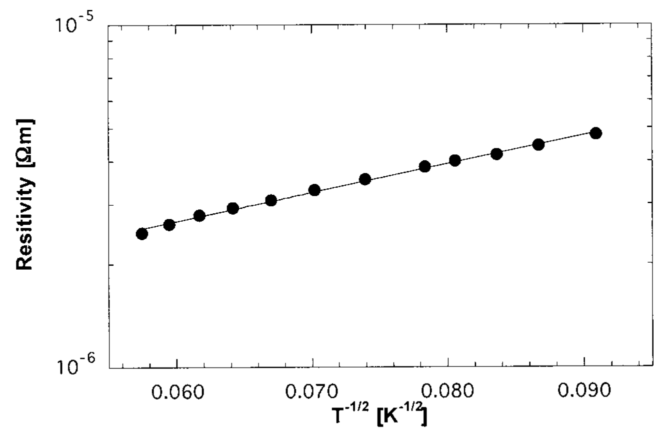

FIG. 2. Temperature dependence of the resistivity for a 1 ML Fe film.

III. ELECTRON TUNNELING IN EPITAXIAL Fe NANOCLUSTERS

In the ultrathin film regime Fe forms three dimensional single crystal clusters on GaAs with an average diameter of a few nanometers.[14] Each of these clusters behaves as a ''giant'' spin where the total spin moment is on the order of $2000\,\mu_B$. Moreover, all clusters have a common easy axis direction determined by the interface-induced crystal anisotropy.[15] The thickness range under investigation is also of particular interest since a change in magnetotransport processes can be expected from a film at the percolation threshold.

For films thinner than 4 ML, the Fe islands are still below the coalescence threshold. The electron transport is determined mainly by the undoped GaAs substrate resulting in a nonmetallic negative temperature coefficient of the resistivity ρ when the samples were cooled down from room temperature to 100 K. In particular, the resistivity of a 1 ML Fe film is very well fitted by the expression $\rho\propto\exp[(C/T)^{1/2}]$, where C is a constant depending on the tunneling barrier height (see Fig. 2). The observed temperature dependence is a strong indication that the main mechanism for electron conduction is thermally activated tunneling between metallic clusters.[16,17]

Furthermore, we found with *in situ* MR three different magnetic phases when the films were cooled down from room temperature to 100 K due to the small size. Above 330 K, the majority of the Fe islands are nonmagnetic with a Curie temperature of about 330 K, resulting in a very weak MR response.

In the temperature range of $200\leqslant T\leqslant330$ K, ferromagnetic ordering within each cluster occurs but due to their large separation no ferromagnetic interaction between clusters can be established. Thermally activated, the magnetization of each cluster points in a random direction, causing the superparamagnetic nature of the film.

When the samples were further cooled below 200 K, intercluster ferromagnetic ordering sets in. The longitudinal MR response in the low temperature regime clearly exhibits an anisotropic MR (AMR) as seen in Fig. 3 for a 2.5 ML Fe film at 135 K. The increase of the resistivity with an increasing magnetic field is due to the AMR effect in the ferromag-

Downloaded 28 Nov 2002 to 144.32.136.70. Redistribution subject to AIP license or copyright, see http://ojps.aip.org/japo/japcr.jsp

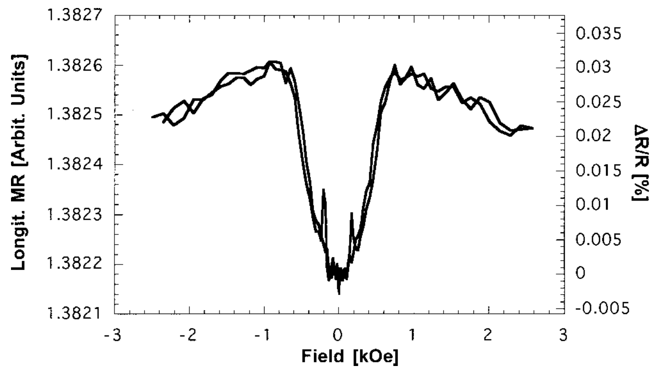

FIG. 3. AMR loop taken from a 2.5 ML Fe film on GaAs at 135 K.

netically ordered Fe clusters. For magnetic fields larger than 1 kOe, a decrease in resistivity with an increasing applied field is seen (see Fig. 3). This can be explained in terms of a superimposed AMR with a ''tunnel magnetoresistance (TMR)-like'' signal.

The decrease of the resistivity with an increasing magnetic field is a characteristic of TMR as occurs in ferromagnetic nanoparticles embedded in an insulating matrix.[18] Due to a distribution in cluster size in our samples, there is a coexistence of ferromagnetic ordered clusters with superparamagnetic clusters at a fixed temperature. At higher magnetic fields the TMR-like effect of the superparamagnetic clusters dominates the MR response and therefore decreases the resistivity.

An important question is whether the tunneling between nanoparticles occurs via the vacuum or via the substrate. In these structures, the Schottky barrier arises at the Fe/GaAs interface leading to a barrier height of ≈0.7 eV. On the other hand, the vacuum level is at ≈4.5 eV above the Fermi energy E_F. Therefore we conclude that tunneling via the GaAs substrate is likely to be the dominant process since in each case the separation between clusters is ≈2 nm and so only the barrier height determines the probability for tunneling.

The appearance of an AMR signal clearly marks the vanishing of the superparamagnetic phase and the onset of ferromagnetic ordering between clusters. Fitting a Langevin function to the magneto-optic Kerr effect (MOKE) loops measured from these films, we estimated the island diameter to be on the order of 5 nm. The cluster size agrees well with STM images obtained from 2.3 ML Fe on InAs for which a similar growth mode is found.[15] The observed superparamagnetic to ferromagnetic transition is in agreement with MOKE results already reported by Xu *et al.*[14] After the deposition of more than 3 ML Fe, the transition from the superparamagnetic to the ferromagnetic phase is complete, the TMR-like signal vanishes and the AMR signal is clearly established, as expected for a continuous film.

IV. SPIN DETECTION IN THE FM/SC SCHOTTKY DIODE STRUCTURES

From the $I-V$ curves obtained without photoexcitation we infer that each sample shows clear Schottky characteristics at the FM/SC interface. The ideality factor[19] was calculated to be 6.69, 5.37, and 4.04 for the samples with substrate doping densities of $n=10^{23}$, 10^{24}, and $p=10^{25}\,\mathrm{m}^{-3}$, respectively. These samples also contain weak ohmic components, which gives rise to a degree of linearity in the $I-V$ curves around zero bias. With increasing doping density, the Schottky barrier height ϕ_b is observed to decrease from approximately 0.8 ($n=10^{23}\,\mathrm{m}^{-3}$) to 0.2 eV ($p=10^{25}\,\mathrm{m}^{-3}$) in the NiFe/GaAs hybrid structures as expected.[13] Because a significant Schottky barrier is seen with $n=10^{23}\,\mathrm{m}^{-3}$, we mainly discuss results from this sample.

The helicity-dependent photocurrent I was measured by modulating the photon helicity from right ($\boldsymbol{\sigma}^+$) to left ($\boldsymbol{\sigma}^-$) using a photoelastic modulator operated at 50 kHz and then detected as an ac signal using lock-in techniques. This method enables us to obtain helicity-dependent effects independent of any background dc currents. The two helicity values correspond to opposite spin angular momentum values of the incident photons which give rise to opposite spin polarizations of electrons photoexcited in the GaAs. For the polarized illumination mode, the bias dependence of the ac helicity-dependent photocurrent I through the interface was probed both (a) in the remanent state ($H=0$, I^0) and (b) under the application of a magnetic field ($H=1.8\,\mathrm{T}$) sufficient to saturate the magnetization along the plane normal (I^n). Consequently, for the configuration $\boldsymbol{\sigma}\|\mathbf{M}$, the NiFe layers are expected to behave as a spin filter due to the spin polarization at the Fermi level E_F,[20] i.e., only minority spin electrons contribute to the transmitted current. In this case, only electrons with minority spin can enter the FM metal from the SC, which means a greater net negative current now flows (compared with that for $\boldsymbol{\sigma}\perp\mathbf{M}$). Spin filtering is therefore turned on or off by controlling the relative axes of $\boldsymbol{\sigma}$ and $\mathbf{M}$, and detected as the helicity-dependent photocurrent I. With $\boldsymbol{\sigma}\perp\mathbf{M}$, I^0, there is no spin filtering, while spin filtering is turned on by rotating to $\boldsymbol{\sigma}\|\mathbf{M}$, I^n.

In our experiment, we measure the helicity-dependent photocurrents I^0 and I^n, which are proportional to the difference between the current components for right ($\boldsymbol{\sigma}^+$) and left ($\boldsymbol{\sigma}^-$) circularly polarized light for each magnetization configuration: $I^0=p^0|i_0^+-i_0^-|$ and $I^n=p^n|i_n^+-i_n^-|$, where p^0 and p^n are phase factors for $\boldsymbol{\sigma}\perp\mathbf{M}$ and $\boldsymbol{\sigma}\|\mathbf{M}$, respectively. Since the auto-phase mode was used for these measurements, the phase factor was optimized in each case. As shown in Fig. 4, $i_0^+=i_0^-$ is expected for the case of the remanent states, while $i_n^+\neq i_n^-$ is expected for perpendicular saturation due to the spin polarization of the density of states at the Fermi level in the FM. In principle, the helicity-dependent photocurrent I^0 should be zero and I^n should reflect the electron spin polarization both in the SC and the FM, i.e., we expect $|I^0|<|I^n|$.

Typical helicity-dependent photocurrent curves are shown in Fig. 4(a) for the case of the $n=10^{23}\,\mathrm{m}^{-3}$ doped sample with $h\nu=1.59\,\mathrm{eV}$. An almost constant difference between the helicity-dependent photocurrent for the two configurations ($\Delta I=I^n-I^0$) is seen at negative bias, which corresponds to the spin-polarized photocurrent passing predominantly from the SC to the FM with a transmitted intensity dependent on the magnetization configurations as discussed above [see Fig. 4(b)]. Minor increases in both I^0 and I^n are obtained with increasing bias which resemble the

Downloaded 28 Nov 2002 to 144.32.136.70. Redistribution subject to AIP license or copyright, see http://ojps.aip.org/japo/japcr.jsp

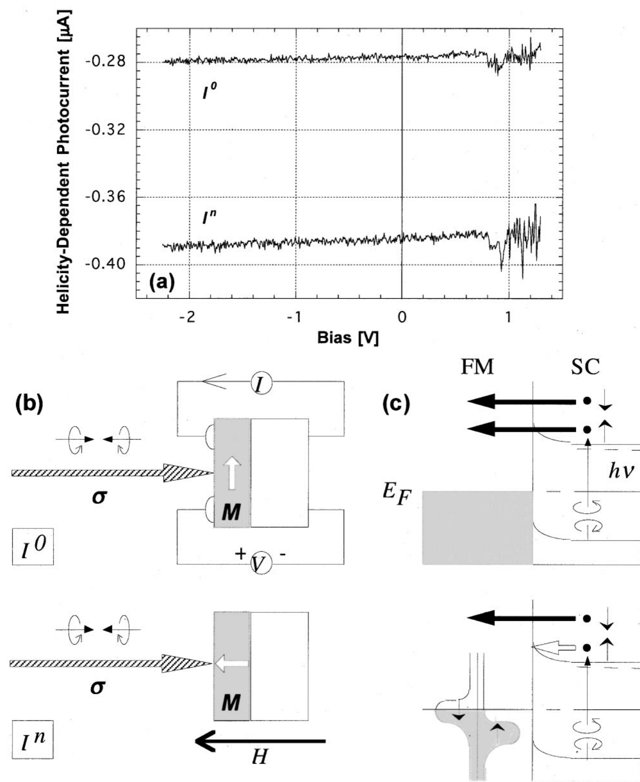

FIG. 4. (a) Bias dependence of the helicity-dependent photocurrent without (I^0) and with (I^n) the applied magnetic field in the case of NiFe/GaAS (100) ($n = 10^{23}\ \mathrm{m}^{-3}$) induced by photoexcitation ($h\nu = 1.59$ eV). Schematic diagrams illustrating (b) the $\boldsymbol{\sigma}$,**M** configurations and (c) the spin filtering mechanism for photoexcited electron transport at the FM/SC Schottky interface.

form of the usual $I-V$ characteristic seen without photoexcitation. It is very important to note that the helicity-dependent photocurrent values for $\boldsymbol{\sigma}\perp\mathbf{M}(I^0)$ and $\boldsymbol{\sigma}\|\mathbf{M}(I^n)$ configurations are observed to satisfy $|I^0|<|I^n|$.

We propose a simple model to explain the spin filtering as shown schematically in Fig. 4(c). Valence band electrons in the SC are first excited into the conduction band by the circularly polarized light and then tunnel through the Schottky barrier into the FM. The photoexcited electrons in the conduction band are partially spin polarized, according to the helicity $\boldsymbol{\sigma}$, due to the dipole selection rules.[21] In the remanent state [top panel of Fig. 4(c)], since the magnetization in the FM is orthogonal to the photoexcited spin polarization, both up and down spin-polarized electrons in the SC can flow into the FM, opposing the electron current from the FM. At perpendicular saturation ($\boldsymbol{\sigma}\|\mathbf{M}$) [bottom panel of Fig. 4(c)], on the other hand, the up spin electron current from the SC is filtered due to the spin split density of states at the Fermi level E_F of the FM, i.e., only minority states are available to electrons tunneling from the SC. This means that a strong difference between the up and down spin currents occurs at perpendicular saturation. The observation that $|I^0| < |I^n|$ provides clear evidence that spin-polarized transport from the SC to the FM occurs under the application of a perpendicular magnetic field. Surprisingly, I^0 is offset from the zero value predicted by our simple model. Such an offset is seen only in NiFe structures, and is not seen for Fe or Co,

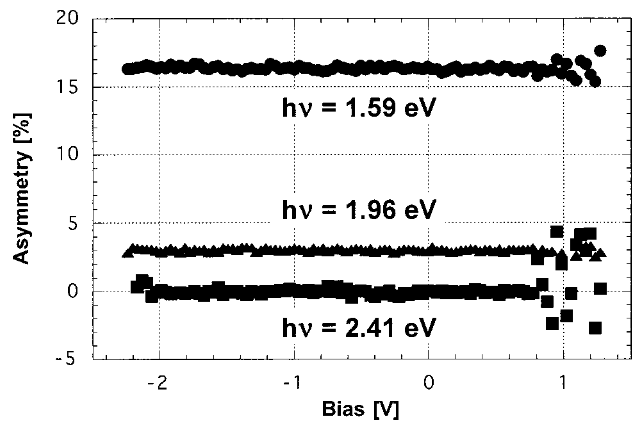

FIG. 5. Bias dependence of asymmetry with NiFe/GaAs (100) ($n = 10^{23}\ \mathrm{m}^{-3}$) induced by the photon energy of $h\nu = 1.59$ (circular dots), 1.96 (triangles), and 2.41 eV (squares).

indicating that the offset is not associated with any experimental asymmetry.

In GaAs, when $h\nu = E_g = 1.43$ eV (E_g is the energy gap in GaAs), the maximum spin polarization is expected to be approximately 40%.[21,22] For $E_g + \Delta < h\nu$ ($\Delta = 0.34$ eV, the valence band splitting in GaAs), the spin polarization decreases due to transitions from the split-off valence band states, which contribute oppositely to the sign of the conduction band spin polarization. Pierce and Meier performed photoemission measurements and found the maximum spin polarization of 44% for $h\nu = 1.5$ eV close to the value of 50% theoretically predicted.[21] With increasing photon energy, the conduction band spin polarization reduces as expected. To quantify the polarization in our experiments, an asymmetry A is introduced as a measure of the spin polarization of the photoexcited electron current where $A = (I^n - I^0)/(I^n + I^0)$.

The bias dependence of the asymmetry A is shown in Fig. 5 for three photon energies $h\nu = 1.59$, 1.96, and 2.41 eV. At each photon energy, A is found to be almost constant for $V < \phi_b$. A also decreases from 16% ($h\nu = 1.59$ eV) to 0% ($h\nu = 2.41$ eV) with increasing photon energy, which indicates that the photoinduced spin polarization in the SC vanishes at high photon energy as discussed above. These results

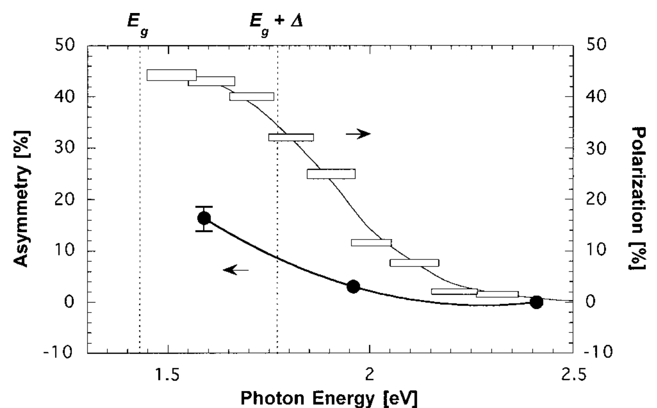

FIG. 6. Photon energy dependence of asymmetry at $V = 0$ V for the case of $n = 10^{23}\ \mathrm{m}^{-3}$ doped sample (circular dots). The spin polarization in GaAs measured by photoemission (rectangles) is also shown (see Ref. 21).

Downloaded 28 Nov 2002 to 144.32.136.70. Redistribution subject to AIP license or copyright, see http://ojps.aip.org/japo/japcr.jsp

indicate that the observed asymmetry A is indeed consistent with our model, i.e., the spin polarization of the photoexcited electrons is determined by the photon energy and spin filtering by the FM films occurs independently of the photon energy. Furthermore, the contribution from magnetic circular dichroism effects associated with the propagation of the laser light through the magnetic film is calculated to be approximately 0.2%,[13] which is much smaller than the observed value of A (4.5% with $n=10^{24}\,\mathrm{m}^{-3}$ and $h\nu=1.96\,\mathrm{eV}$, for instance), and is therefore negligible. This suggests that there are no other processes that could mimic this asymmetry.

Figure 6 shows that the asymmetry A at zero bias increases with decreasing photon energy $h\nu$ for $n=10^{23}\,\mathrm{m}^{-3}$ doped substrates. The spin polarization curve for GaAs obtained by photoemission is also shown for Ref. 21. A clear trend is observed with increasing A as the photon energy $h\nu$ decreases and approaches E_g. Moreover, the magnitude of the asymmetry A reaches 16% at the smallest photon energy, which agrees well with the order of magnitude of the polarization estimated from the photoemission experiment. According to Julliere's model,[23] the spin polarization across a tunnel barrier can be estimated as $P=2P_1P_2/(1+P_1P_2)$ where P_1 and P_2 are the spin polarizations of the two FM layers. Since we assume spin-polarized electron tunneling across the FM/SC interface, we apply this model to our system. Using $P_1=43\%$ for GaAs at $h\nu=1.59\,\mathrm{eV}$[21] and P_2 of 45% for NiFe,[20] the maximum spin polarization P can be deduced to be 32%. Considering that the asymmetry A is observed to be 16% as $h\nu=1.59\,\mathrm{eV}$, the efficiency of our spin detection can be estimated to be approximately 50% at room temperature. This value indicates that spin-polarized electrons are transmitted from the SC to the FM with high efficiency, although a precise correspondence cannot be expected since A is not a true measure of the electron polarization P. Since a large spin polarization occurs at E_F in the NiFe,[20] NiFe may be a particularly appropriate metal for such studies.

V. CONCLUSION

The lateral size and interface magnetism in the FM/SC hybrid structures have been assessed. *In situ* magnetoresistance was used to investigate the electrical transport properties of ultrathin epitaxial Fe films deposited on GaAs (100) substrates. For the cluster phase, it was found that the main mechanism for electron conduction is thermally activated tunneling between the epitaxial Fe nanoparticles. These clusters are predominately superparamagnetic just below room temperature ($T\approx 250\,\mathrm{K}$) giving rise to a TMR-like magnetoresistance. At low temperatures ($T\approx 100\,\mathrm{K}$) the Fe clusters establish ferromagnetic order and therefore exhibit the well-known AMR. We infer from the photoexcitation results that the presence of the Schottky barrier is of key importance for the spin transport behavior in these Fe nanoclusters since it is likely that spin detection occurs due to the same spin filtering process identified in the NiFe/GaAs structures.

We have also found that efficient spin-polarized electron transport occurs across the NiFe/GaAs interface. Strong spin filtering in the ferromagnetic NiFe layer reduces the transmission of photoexcited spin-polarized electrons tunneling from the SC to the FM when the FM magnetization is aligned with the photon helicity. The photocurrent asymmetry approaches 20% for the smallest photon energy used and is expected to increase still further as the photon energy approaches the SC band gap, which holds promise for the development of spin electronic devices. This result is likely to be significant in the development of future spin electronic devices based on the combination of hybrid FM/SC structures.

ACKNOWLEDGMENTS

The authors are grateful to Dr. Stuart Holmes for assistance with the sample preparation. The support of EPSRC and EU (MASSDOTS project) is also acknowledged. A. H. would like to thank Toshiba Europe Research Limited for their financial support.

[1] G. A. Prinz, J. Magn. Magn. Mater. **200**, 57 (1999).
[2] M. Johnson, IEEE Spectrum **37**, 33 (2000).
[3] S. Datta and B. Das, Appl. Phys. Lett. **56**, 665 (1990).
[4] R. Fiederling, M. Keim, G. Reunscher, W. Ossau, G. Schmidt, A. Waag, and L. W. Molenkamp, Nature (London) **402**, 787 (1999).
[5] Y. Ohno, D. K. Young, B. Beschoten, F. Matsukura, H. Ohno, and D. D. Awschalom, Nature (London) **402**, 790 (1999).
[6] I. Malajovich, J. M. Kikkawa, D. D. Awschalom, J. J. Berry, and N. Samarth, Phys. Rev. Lett. **84**, 1015 (2000).
[7] M. Johnson and R. H. Silsbee, Phys. Rev. Lett. **55**, 1790 (1985).
[8] P. R. Hammar, B. R. Bennet, M. J. Yang, and M. Johnson, Phys. Rev. Lett. **83**, 203 (1999).
[9] G. Schmidt, D. Ferrand, L. W. Molenkamp, A. T. Filip, and B. J. van Wees, Phys. Rev. B **62**, R4790 (2000).
[10] R. Fitsgerald, Phys. Today **53**, 21 (2000).
[11] C. M. Gürtler, Y. B. Xu, and J. A. C. Bland, J. Magn. Magn. Mater. (in press).
[12] M. W. J. Prins, H. van Kempen, H. van Leuken, R. A. de Groot, W. van Roy, and J. de Boeck, J. Phys.: Condens. Matter **7**, 9447 (1995).
[13] A. Hirohata, Y. B. Xu, C. M. Guertler, and J. A. C. Bland, J. Appl. Phys. **87**, 4670 (2000).
[14] Y. B. Xu, E. T. M. Kernohan, D. J. Freeland, A. Ercole, M. Tselepi, and J. A. C. Bland, Phys. Rev. B **58**, 890 (1998).
[15] Y. B. Xu, D. J. Freeland, M. Tselepi, and J. A. C. Bland, J. Appl. Phys. **87**, 6110 (2000).
[16] P. Sheng, B. Abeles, and Y. Arie, Phys. Rev. Lett. **31**, 44 (1973).
[17] J. S. Helman and B. Abeles, Phys. Rev. Lett. **37**, 1429 (1976).
[18] J. I. Gittleman, Y. Goldstein, and S. Bozowski, Phys. Rev. B **5**, 3609 (1972).
[19] S. M. Sze, *Physics of Semiconductor Devices*, 2nd ed. (Wiley, New York, 1981), pp. 245–311.
[20] B. Nadgorny *et al.*, Phys. Rev. B **61**, R3788 (2000).
[21] D. T. Pierce and F. Meier, Phys. Rev. B **13**, 5484 (1976).
[22] S. Adachi, *GaAs and Related Materials* (World Scientific, Singapore, 1994), pp. 145.
[23] M. Julliere, Phys. Rep. **54A**, 225 (1975).

Downloaded 28 Nov 2002 to 144.32.136.70. Redistribution subject to AIP license or copyright, see http://ojps.aip.org/japo/japcr.jsp